JACS
JOURNAL OF THE AMERICAN CHEMICAL SOCIETY

Article

pubs.acs.org/JACS

Role of Water in Stabilizing Ferricyanide Trianion and Ion-Induced Effects to the Hydrogen-Bonding Water Network at Long Distance

Matthew J. DiTucci, Sven Heiles,[§] and Evan R. Williams*

Department of Chemistry, University of California, Berkeley, California 94720-1460, United States

Supporting Information

ABSTRACT: Structures and reactivities of gaseous $Fe(CN)_6^{3-}(H_2O)_n$ were investigated using infrared photodissociation (IRPD) kinetics, spectroscopy, and computational chemistry in order to gain insights into how water stabilizes highly charged anions. $Fe(CN)_6^{3-}(H_2O)_8$ is the smallest hydrated cluster produced by electrospray ionization, and blackbody infrared dissociation of this ion results in loss of an electron and formation of smaller dianion clusters. $Fe(CN)_6^{3-}(H_2O)_7$ is produced by the higher activation conditions of IRPD, and this ion dissociates both by loss of an electron and by loss of a water molecule. Comparisons of IRPD spectra to those of computed low-energy structures for $Fe(CN)_6^{3-}(H_2O)_8$ indicate that water molecules either form two hydrogen bonds to the trianion or form one hydrogen bond to the ion and one to another water molecule. Magic numbers are observed for $Fe(CN)_6^{3-}(H_2O)_n$ for n between 58 and 60, and the IRPD spectrum of the $n = 60$ cluster shows stronger water molecule hydrogen-bonding than that of the $n = 61$ cluster, consistent with the significantly higher stability of the former. Remarkably, neither cluster has a band corresponding to a free O−H stretch, and this band is not observed for clusters until $n \geq 70$, indicating that this trianion significantly affects the hydrogen-bonding network of water molecules well beyond the second and even third solvation shells. These results provide new insights into the role of water in stabilizing high-valency anions and how these ions can pattern the structure of water even at long distances.

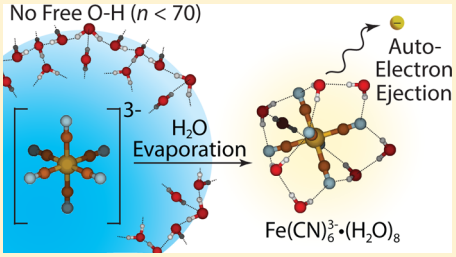

INTRODUCTION

High-valency ions are common in solution, where surrounding water or other solvent molecules can stabilize the charge.[1] Large, multiply charged molecules, such as those produced by electrospray ionization of proteins, DNA, carbohydrates, or other large molecules, can be very stable, even without solvent, owing to high intrinsic charge affinities and to the typically large separation distances between charges.[2−5] Much smaller, multiply charged species, such as multivalent atomic ions or those formed from small molecules, are much more reactive owing to significant Coulomb energy in the bare ions.[6−30] In the gas phase, these ions often either spontaneously dissociate in charge-separation reactions[9−14,17−22] or transfer charge to other molecules in collisions, e.g., proton transfer.[23]

The reactivities of highly charged small molecular and atomic ions have been extensively investigated.[6−41] Schwarz and co-workers found that the product ions, $Cu^+ + X^+$ ($X = H_2O$, NH_3) formed by charge separation of $Cu(X)^{2+}$ ($X = H_2O$, NH_3), are thermodynamically more stable but $Cu(X)^{2+}$ is metastable because of a Coulomb barrier.[35] A Coulomb barrier in the charge-separation reactions of multiply charged ions, both positive and negative, arises from the combined potentials for short-range binding interactions and long-range charge−charge repulsion.[3,4,29−31] The stabilities of highly charged ions can be enhanced by solvation. For example, isolated SO_4^{2-} is unstable with respect to electron loss with a calculated lifetime of 1.6×10^{-10} s.[34] However, this ion can be stabilized by water molecules and can be observed in the form of hydrated clusters, $SO_4^{2-}(H_2O)_n$. Wang and co-workers showed through photoelectron spectroscopy (PES) studies that each additional water molecule increases the barrier for electron loss.[39,40] Extrapolation of these PES data to small cluster sizes indicated that clusters with $n = 1$ and 2 are electronically unstable by −0.9 and −0.2 eV, respectively, in excellent agreement with computed values.[15] From these results, Wang and co-workers concluded that three water molecules are necessary to stabilize SO_4^{2-}. Blades and Kebarle reported formation of $SO_4^{2-}(H_2O)_2$ indicating that this species has a sufficient lifetime to be observed in a mass spectrometer.[13]

For bare multivalent cations, charge separation to form protonated water or protonated water clusters can occur upon the sequential addition of water molecules.[25−28] Addition of a water molecule to $Ca^{2+}(H_2O)$ results in the formation of $CaOH^+$ and H_3O^+, a reaction that can occur through a $M^{2+}-OH^--H_3O^+$ salt-bridge intermediate structure.[27] For this reason, large hydrated clusters of many multivalent ions cannot be formed by condensing water molecules sequentially onto the bare ion.

Extensively hydrated multiply charged ions can be readily formed by electron ionization of singly charged clusters[32,33] or by electrospray ionization,[21,42,43] and these methods provide an excellent means by which to investigate the role of water in stabilizing multivalent ions. Evaporation of water molecules

Received: November 21, 2014
Published: January 8, 2015

DOI: 10.1021/ja5119545
J. Am. Chem. Soc. 2015, 137, 1650−1657

from large clusters can result in charge-separation reactions at smaller cluster size. For multivalent anions, charge separation can occur either by electron loss or by loss of OH^- or $OH^-(H_2O)_n$.[12−14] The cluster size at which charge separation competes with the loss of a water molecule depends on the internal energy of the cluster and the identity of the ion. For example, blackbody infrared dissociation (BIRD) of $SO_4^{2-}(H_2O)_n$ at 21 °C results predominantly in loss of a water molecule for $n \geq 6$, but predominantly in charge separation for $n = 5$.[12] However, loss of a water molecule is entropically favored,[12] and smaller clusters of SO_4^{2-} can be produced by using more energetic activation conditions.

The smallest cluster for which a multivalent ion is observed has often been referred to as the critical size, n_c, and a number of values for different ions have been reported. Critical cluster sizes for the dications, such as Zn^{2+}, Co^{2+}, Be^{2+}, and Cu^{2+}, range from ∼2 to 7,[18−20] and for trivalent cations, such as Ce^{3+}, La^{3+}, Tb^{3+}, and Lu^{3+}, from ∼15 to 18.[21,22] Significantly more water molecules are required to stabilize the higher charge density on trivalent monoatomic ions compared to that of the divalent monoatomic ions. Because the observed cluster size of hydrated multivalent ions depends on the internal energy that is deposited into larger clusters as well as the lifetime of the ion, a more consistent definition of critical size as the cluster size at which charge separation is energetically favored over the loss of one water molecule has been proposed.[20]

Here, the dissociation pathways of hydrated clusters of the small trianion ferricyanide, $Fe(CN)_6^{3-}(H_2O)_n$, are investigated using BIRD, infrared photodissociation (IRPD), spectroscopy, and computational chemistry. Although $Fe(CN)_6^{3-}(H_2O)_8$ is the smallest cluster observed in electrospray ionization mass spectra under a wide variety of conditions, clusters with seven water molecules are stable when larger clusters are activated with photons generated by an IR laser, and evidence for clusters with six water molecules is presented. For these small clusters, charge separation occurs via electron loss. Although both bare $P_3O_9^{3-}$ and $Co(NO_2)_6^{3-}$ have been reported previously,[44] these ions are not formed under identical conditions for successfully generating $Fe(CN)_6^{3-}(H_2O)_n$. We find that $P_3O_9^{3-}$ is only observed with six or more water molecules attached, and this ion undergoes charge separation to form $HP_3O_9^{2-}(H_2O)_5 + OH^-$. This is the first report of a critical cluster size for small trianions, and these are the smallest trianions (highest charge density) that have been observed in the gas phase.

EXPERIMENTAL METHODS

All experimental data were obtained using a home-built Fourier transform ion cyclotron resonance (FT-ICR) mass spectrometer that is described elsewhere[45] and has been upgraded to incorporate a 7 T magnet. Hydrated ions are formed by nanoelectrospray ionization (nESI) of 5 mM aqueous solutions of potassium ferricyanide (Matheson Coleman & Bell, Norwood, OH) using a Milli-Q purified water system (Millipore, Billerica, MA). Solutions are loaded into borosilicate capillaries that have tips pulled to an inner diameter of ∼1 μm. A platinum wire that is in contact with the solution is held at a constant potential of ∼700 V with respect to a heated metal capillary at the entrance of the instrument. Ions are guided via electrostatic lenses through five stages of differential pumping into the ion cell, which is enclosed by a copper jacket and is temperature controlled by a regulated flow of liquid nitrogen to 133 K for at least 8 h prior to data acquisition.[46] A pulse of dry nitrogen gas is introduced into the instrument for ∼6 s, bringing the pressure of the vacuum chamber containing the ion cell to $\sim 2 \times 10^{-6}$ Torr, which helps to both trap and thermalize the ions. After an ∼8 s pump down period following the pulse gas, the pressure in the chamber decreases to $\sim 2 \times 10^{-9}$ Torr. Precursor ions of interest are subsequently isolated using a notched stored waveform inverse Fourier transform (SWIFT) excitation.

IRPD spectra between 2900 and 3800 cm^{-1} are measured using infrared photons from a tunable OPO/OPA system (LaserVision, Bellevue, WA) pumped by the 1064 nm fundamental of a Nd:YAG laser (Continuum Surelight I-10, Santa Clara, CA) operating at a 10 Hz repetition rate. Ions are irradiated for between ∼0.5 and 3.0 s in order to produce substantial, but not complete, dissociation of the precursor. A first-order rate constant is derived from the relative abundances of precursor and product ions after photodissociation. BIRD rate constants are obtained from the dissociation of the precursor in the absence of laser irradiation for 0.1−5 s. The IRPD rate constants from laser irradiation are corrected for frequency dependent variations in laser power as well as dissociation due to BIRD.[47]

For double-resonance experiments, a single-frequency excitation matching the cyclotron frequency of the ion to be ejected is continuously applied to the cell after isolation of the precursor and is sustained until just before ion detection. Ions were photodissociated for 2.5 s at 3521 cm^{-1} to produce significant abundances of fragment ions.

Structures of $Fe(CN)_6^{3-}(H_2O)_8$ were generated by initially positioning water molecules around the ion in Macromodel 9.1 (Schrödinger, Inc., Portland, OR). The structures were geometry optimized using Q-Chem 4.0[48] (Q-Chem, Inc., Pittsburgh, PA) at B3LYP/LACVP++** level of theory prior to vibrational frequency and intensity calculations at the same level of theory. Vibrational frequencies were scaled by 0.955 and convolved with a 60 and 15 cm^{-1} fwhm Gaussian for the 3000−3650 and 3650−3800 cm^{-1} regions, respectively.[49] Zero-point energies, enthalpy, and entropy corrections at 133 K were calculated for these structures using unscaled B3LYP/LACVP++** harmonic oscillator vibrational frequencies. Additional optimizations were performed at the MP2 level with the VTZ basis set, and zero-point energies, enthalpy, and entropy corrections were obtained using frequencies and thermochemical parameters from B3LYP/LACVP++**.

RESULTS AND DISCUSSION

Hydrated Ion Formation. Mass spectra obtained by nESI of 5 mM aqueous solutions of $K_3Fe(CN)_6$ (Figure 1) show abundant hydrated ferricyanide trianions, $Fe(CN)_6^{3-}(H_2O)_n$, with n between 8 and ∼350 water molecules. The distribution of hydrated ions can be shifted from smaller (Figure 1a) to larger (Figure 1b) cluster sizes by decreasing the temperature of the entrance capillary, reducing electrostatic potentials applied to source optics, and modifying the excitation waveforms to optimize ion detection in the m/z range of interest. Cluster sizes with $n > 350$ can be formed using even softer conditions. Other ions present in Figure 1a include $Fe(CN)_6^{2-}(H_2O)_n$ with $n = 0-8$, $HFe(CN)_6^{2-}(H_2O)_n$ with $n = 0-22$, $KFe(CN)_6^{2-}(H_2O)_n$ with $n = 0-24$, $Fe(CN)_5^{2-}$, $Fe(CN)_4^{2-}$, and $Fe(CN)_3^-$.

Formation of the bare gaseous trianions, trimetaphosphate ($P_3O_9^{3-}$) and hexanitrocobaltate ($Co(NO_2)_6^{3-}$), has been reported previously.[44] Under the same conditions used to form the hydrated ferricyanide trianions (Figure 1), these other two trianions are not formed as bare species. nESI of a 5 mM aqueous solution of $Na_3P_3O_9$ results in formation of the trianions, $P_3O_9^{3-}(H_2O)_n$ with $n \geq 6$ (Figure S1). Isolation of the $P_3O_9^{3-}(H_2O)_9$ cluster (Figure S2a) and IRPD at 3438 cm^{-1} for 60 s results in fragments corresponding to sequential water molecule loss to $P_3O_9^{3-}(H_2O)_6$ followed by a charge-separation reaction to form $HP_3O_9^{2-}(H_2O)_5$ and subsequent sequential water molecule loss to form $HP_3O_9^{2-}(H_2O)_{1-4}$ (Figure S2b). Although there is a peak in the nESI spectrum at $m/z = 78.96$,

DOI: 10.1021/ja5119545
J. Am. Chem. Soc. 2015, 137, 1650−1657

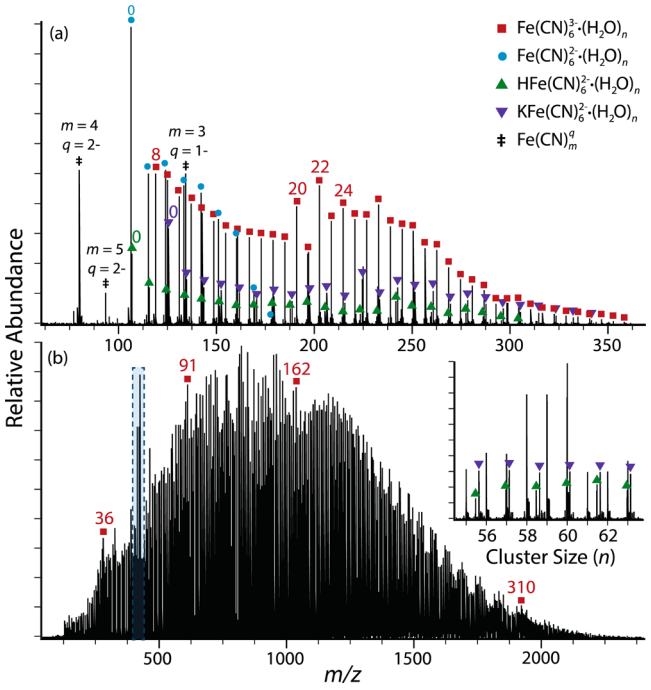

Figure 1. nESI mass spectra obtained from 5 mM aqueous solution of $K_3Fe(CN)_6$ showing formation of $Fe(CN)_6^{3-}(H_2O)_n$, with n between 8 and ~350 under (a) more energetic instrumental conditions to form smaller cluster sizes and (b) soft instrumental conditions to form larger cluster sizes. Inset shows magic number clusters corresponding to $Fe(CN)_6^{3-}(H_2O)_{58-60}$.

which corresponds to that of the bare trianion, the isotope distribution shows that this ion is the dianionic species, $P_2O_6^{2-}$.

These experiments provide compelling evidence that $P_3O_9^{3-}$ is not stable in the gas phase as an isolated ion and likely only exists as a long-lived stable ion with ~6 or more water molecules attached. Similarly, nESI of a 5 mM aqueous solution of $Na_3Co(NO_2)_6$ results in formation of $Co(NO_2)_3^-(H_2O)_n$, $NO_3^-(H_2O)_n$, and $NO_2^-(H_2O)_n$ (Figure S3). We conclude from these experiments that $Fe(CN)_6^{3-}(H_2O)_n$ and $P_3O_9^{3-}(H_2O)_n$ with $n \geq 6$ are the smallest, most highly charged trianions that have been observed to date.

Dissociation Pathways of Ferricyanide Trianion. $Fe(CN)_6^{3-}(H_2O)_8$ is the smallest trianion cluster in the nESI mass spectra obtained using a variety of instrumental conditions. BIRD of $Fe(CN)_6^{3-}(H_2O)_8$ at 133 K for 60 s does not result in observable water loss from the precursor to form $Fe(CN)_6^{3-}(H_2O)_7$ (Figure 2). Instead, there is a product ion corresponding to loss of an electron, $Fe(CN)_6^{2-}(H_2O)_8$ (reaction 1):

$$Fe(CN)_6^{3-}(H_2O)_8 \rightarrow Fe(CN)_6^{2-}(H_2O)_8 + e^- \quad (1)$$

Auto-detachment of an electron was also reported for the following ions: the 3− and 4− charge states of oligonucleotides,[9] sulfonated pyrene trianion,[10] metal phthalocyanine-tetrasulfonate tetraanions,[11] and C_{70}^{2-}.[2] $Fe(CN)_6^{2-}(H_2O)_n$ with n = 0–7 and ions corresponding to ligand loss, $Fe(CN)_4^{2-}$ and $Fe(CN)_3^-$, are also formed by BIRD (Figure 2). Because these complexes are not hydrated, it is likely that the instability of the bare dianion leads to further dissociation through consecutive cyano ligand loss (reactions 2a and 2b). Although $Fe(CN)_5^{2-}$ is not observed with BIRD of $Fe(CN)_6^{3-}(H_2O)_8$, it appears in the electrospray mass spectrum (Figure 1a) but in

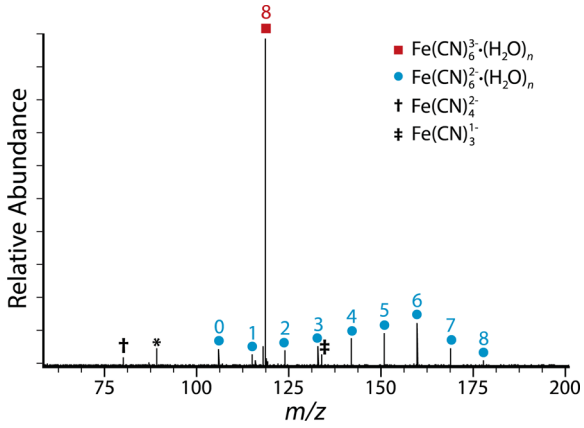

Figure 2. Blackbody infrared radiative dissociation mass spectrum of $Fe(CN)_6^{3-}(H_2O)_8$ at 133 K for 60 s. Frequency noise is labeled with an asterisk (*).

significantly lower abundance than the other two complexes. This indicates that this ion is not very stable or that $Fe(CN)_6^{2-}$ dissociates primarily by loss of $(CN)_2$ to form $Fe(CN)_4^{2-}$, which may occur due to the high enthalpy of formation for $(CN)_2$.[50] $Fe(CN)_4^{2-}$ undergoes a charge-separation reaction to produce $Fe(CN)_3^-$ and CN^- (reaction 2c). The high electron affinity of CN (3.862 eV)[51] likely accounts for the facile formation of CN^-.

$$Fe(CN)_6^{2-} \rightarrow Fe(CN)_5^{2-} + CN \quad (2a)$$

$$Fe(CN)_5^{2-} \rightarrow Fe(CN)_4^{2-} + CN \quad (2b)$$

$$Fe(CN)_4^{2-} \rightarrow Fe(CN)_3^- + CN^- \quad (2c)$$

In order to further elucidate the dissociation pathways of small hydrated trianion ferricyanide, double-resonance experiments were performed for $Fe(CN)_6^{3-}(H_2O)_{10}$ (Figure 3). In these experiments, IRPD at 3521 cm^{-1}, which corresponds to a hydrogen-bonded absorption, is used to vibrationally excite the ions, during which time a single radio frequency excitation at the resonant cyclotron frequency of a possible intermediate in the reaction pathway is applied. Any product ions originating from the continuously ejected ion should not be observed in the mass spectrum if the time scale for their formation is longer than the ~10 μs ejection time.

IRPD of isolated $Fe(CN)_6^{3-}(H_2O)_{10}$ for 2.5 s (Figure 3a) results in formation of $Fe(CN)_6^{3-}(H_2O)_{7-9}$ and $Fe(CN)_6^{2-}(H_2O)_{3-7}$ (Figure 3b). The appearance of $Fe(CN)_6^{3-}(H_2O)_7$ with IRPD, which is not observed in the lower-energy BIRD experiment, indicates that the loss of one water molecule from $Fe(CN)_6^{3-}(H_2O)_8$ is entropically favored over loss of an electron.

Results from a double-resonance experiment in which $Fe(CN)_6^{2-}(H_2O)_6$ is continuously ejected is shown in Figure 3c. Both this ion and all the smaller dianions are absent. This demonstrates that $Fe(CN)_6^{2-}(H_2O)_{3-5}$ are formed by sequential water loss from $Fe(CN)_6^{2-}(H_2O)_6$ (reaction 3):

$$Fe(CN)_6^{2-}(H_2O)_n \rightarrow Fe(CN)_6^{2-}(H_2O)_{n-1} + H_2O \quad (3)$$

Continuous ejection of $Fe(CN)_6^{3-}(H_2O)_7$ (Figure 3d) results in the elimination of all dianion products. This suggests that loss of an electron from $Fe(CN)_6^{3-}(H_2O)_n$ with n > 7 contributes negligibly to the formation of hydrated dianions under these more energetic dissociation conditions.

DOI: 10.1021/ja5119545
J. Am. Chem. Soc. 2015, 137, 1650–1657

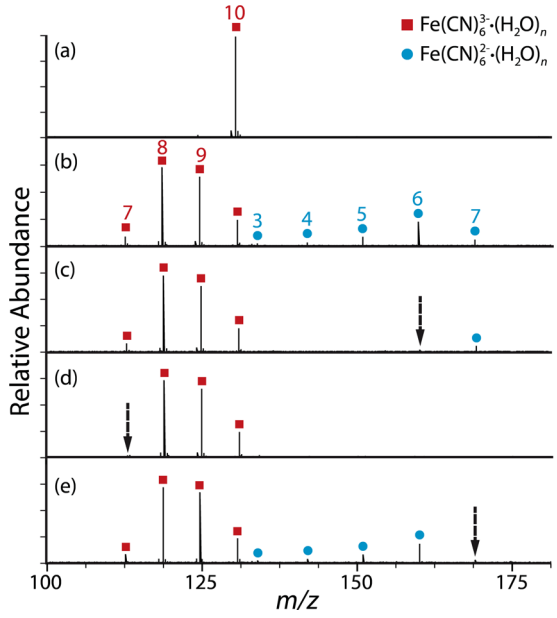

Figure 3. IRPD dissociation and double-resonance data on $Fe(CN)_6^{3-}(H_2O)_{10}$ showing (a) isolated precursor, $Fe(CN)_6^{3-}(H_2O)_{10}$, (b) IRPD of $Fe(CN)_6^{3-}(H_2O)_{10}$ at 3521 cm^{-1} for 2.5 s with double-resonance ejection of possible intermediates corresponding to (c) $Fe(CN)_6^{2-}(H_2O)_6$, (d) $Fe(CN)_6^{3-}(H_2O)_7$, and (e) $Fe(CN)_6^{2-}(H_2O)_7$. Dotted arrows indicate the m/z corresponding to the frequency excited during the experiment.

When $Fe(CN)_6^{2-}(H_2O)_7$ is continuously ejected from the cell, some $Fe(CN)_6^{2-}(H_2O)_{3-6}$ still remain (Figure 3e). This indicates that there is a second dissociation pathway for $Fe(CN)_6^{3-}(H_2O)_7$. To form the $n = 6$ dianion without water loss from the $n = 7$ dianion, electron ejection must occur from $Fe(CN)_6^{3-}(H_2O)_6$, which must have a lifetime that is shorter than the time required for detection in these experiments. These results indicate that the smallest observed hydrate of ferricyanide, $Fe(CN)_6^{3-}(H_2O)_7$, can dissociate via two pathways, either by loss of a neutral water molecule (reaction 4a) or by loss of an electron (reaction 4b):

$$Fe(CN)_6^{3-}(H_2O)_7 \rightarrow Fe(CN)_6^{3-}(H_2O)_6 + H_2O \quad (4a)$$

$$Fe(CN)_6^{3-}(H_2O)_7 \rightarrow Fe(CN)_6^{2-}(H_2O)_7 + e^- \quad (4b)$$

$Fe(CN)_6^{3-}(H_2O)_8$ is the smallest cluster observed in the nESI mass spectra. The absence of $Fe(CN)_6^{3-}(H_2O)_7$ in the BIRD spectrum of $Fe(CN)_6^{3-}(H_2O)_8$ indicates that the lowest-energy dissociation process for this ion is loss of an electron. Sequential loss of water molecules as well as electron loss from the smaller clusters occurs with the higher-energy activation conditions of the IRPD experiments. This indicates that although smaller trianion clusters may be formed under even higher-energy activation conditions, $n = 8$ is the "critical" size where charge separation occurs and appears to be energetically favored over the loss of a water molecule.

Infrared Photodissociation Spectroscopy of $Fe(CN)_6^{3-}(H_2O)_8$. In order to gain insight into the structure of $Fe(CN)_6^{3-}(H_2O)_8$, the smallest trianion formed directly by nESI, an IRPD spectrum in the hydrogen oscillator region from 3100 to 3800 cm^{-1} was obtained (Figure 4a). The vibrational modes for the O−H stretch of water are sensitive to the local hydrogen-bonding environment and can provide information about how water molecules organize around the ion.

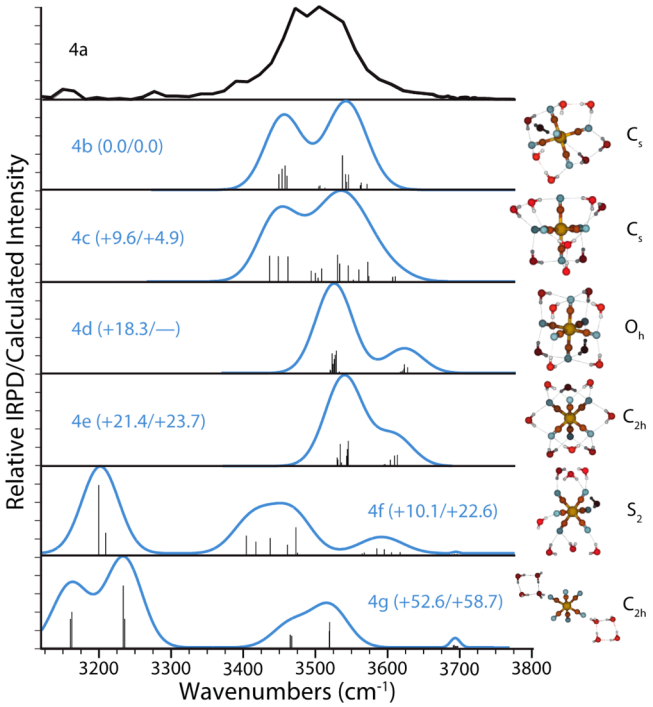

Figure 4. Spectra of $Fe(CN)_6^{3-}(H_2O)_8$. (a) IRPD spectrum and (b–g) calculated spectra and corresponding optimized structures calculated at the B3LYP/LACVP++** level. Gibbs free energies (in kJ/mol at 133 K) relative to the lowest-energy structure **4b** are inset with values from B3LYP/MP2. Point groups for calculated structures are provided on the right.

The IRPD spectrum of $Fe(CN)_6^{3-}(H_2O)_8$ (Figure 4a) has a broad band that appears to be comprised of at least two separate absorption bands centered at 3471 and 3505 cm^{-1}. Two low-intensity absorptions at 3150 and 3270 cm^{-1} are within baseline noise in this region of the spectrum, where both the laser power and photon energy are lower. This region of the spectrum corresponds to bonded O−H stretches indicative of water molecules that donate a hydrogen bond to another atom. There is no peak in the free O−H region, which indicates that both of the hydrogen atoms for all eight water molecules are hydrogen-bonded either to $Fe(CN)_6^{3-}$ or to other water molecules.

Calculated low-energy structures and corresponding IR spectra for $Fe(CN)_6^{3-}(H_2O)_8$ are shown in Figure 4 (**4b**–**4g**). The lowest-energy structure, **4b**, has four pairs of water molecules that bridge between three cyano ligands. One water molecule in the pair hydrogen bonds to a cyano group and to the oxygen atom of an adjacent water molecule (double donor, or DD, water molecule). This adjacent water molecule hydrogen bonds directly to two cyano groups and accepts one hydrogen bond from the paired water molecule (acceptor–donor–donor, or ADD, water molecule). Structure **4b** contains four of these pairs of water molecules, whereas structure **4c** (+9.6/+4.9 kJ/mol with B3LYP/MP2 energies, respectively) has three of these pairs and two water molecules that bond to two cyano groups (DD). The spectra for **4b** and **4c** have bonded O−H stretches between ~3350 and 3650 cm^{-1}, which match well with the experimental spectrum.

Structures **4d** and **4e** are higher-energy structures that share the same structural motif in that each water molecule donates two hydrogen bonds to nitrogen atoms of adjacent cyano ligands. These structures have no water–water hydrogen

DOI: 10.1021/ja5119545
J. Am. Chem. Soc. 2015, 137, 1650–1657

bonds. The calculated spectra have two bonded O−H bands corresponding to symmetric/asymmetric vibrations at 3527/3625 and 3541/3606 cm^{-1} for **4d** and **4e**, respectively. These stretches are blue-shifted from those in the experimental spectrum. In addition, these structures are >18 kJ/mol higher in energy (structure **4d** converged to a different structure at the MP2/VTZ level, **4h** (Figure S4), which has a free O−H stretch and is 14.3 kJ/mol higher in energy), indicating that these isomers are not present.

Some CN ligands in structure **4f** (>+10 kJ/mol) are involved in a single hydrogen bond to just one water molecule, and two water molecules have a free O−H stretch. There is no free O−H stretch in the IRPD spectrum, although this is not calculated to be an intense feature. A structure in which water forms two rings, **4g**, is not energetically favorable (>+50 kJ/mol) and should have a free O−H stretch band at 3697 cm^{-1} that is not observed experimentally. Based on comparisons between the calculated spectra and the measured IRPD spectrum as well as the computed energies, structures **4b** and **4c** are likely to be the predominant structures in these experiments.

The CN ligands in both structures **4b** and **4c** each interact with at least two water molecules. Removal of a single water molecule from either structure results in a CN ligand that accepts a hydrogen bond from just one water molecule. Such a structure is not energetically favorable to form under the low-energy conditions of nESI or dissociation by BIRD, but can be formed by more energetic activation of larger clusters.

Magic Number Clusters. The abundance of a cluster depends on its stability as well as the stabilities of larger clusters. Clusters with anomalously high abundances are commonly referred to as magic number clusters. For $Fe(CN)_6^{3-}(H_2O)_n$, n between 58 and 60 are magic number clusters (Figure 1b) and, to a lesser extent, n = 20 and 22 are as well (Figure 1a).

To determine if the high abundances of the larger magic number clusters are associated with high ion stabilities or exceptional instability in the $n + 1$ clusters, BIRD dissociation constants were measured for n = 56−62. The BIRD rate constant for n = 60 (k_{BIRD} = 0.088 s^{-1}) is significantly lower than that for n = 61 (k_{BIRD} = 0.36 s^{-1}) or n = 62 (k_{BIRD} = 0.49 s^{-1}). This suggests a stable core structure is established for n = 60, and that additional water molecules do not bind strongly to or disturb this core structure. Magic number clusters around this size have also been reported for $(H_2O)^-_n$ and $H^+(H_2O)_n$ for alternating cluster sizes,[42,52−54] whereas ferricyanide has three successive clusters with higher abundance.

In order to gain further insight into the unusual stabilities of these ions, an IRPD spectrum of $Fe(CN)_6^{3-}(H_2O)_{60}$ was compared to that of the significantly less stable $Fe(CN)_6^{3-}(H_2O)_{61}$ (Figure 5). The bonded O−H region of the n = 60 cluster has a broad peak centered at 3438 cm^{-1} with an apparent shoulder at ~3550 cm^{-1}. The maximum of this absorption is at a slightly higher frequency for the n = 61 cluster. The red shift in the spectrum for the n = 60 cluster is indicative of stronger, more optimal hydrogen bonding and is consistent with the higher stability of this cluster. The shoulder at ~3550 cm^{-1} has previously been attributed to three-coordinate ADD water molecules for some clusters.[55−59] There is a strong ADD stretch in the spectra of $Cs^+(H_2O)_{20}$ and some other alkali metal ions that is indicative of clathrate structures.[58,60] This band in $Fe(CN)_6^{3-}(H_2O)_{60}$ may indicate the possibility of similar complex cage-like structures. Remarkably, there is not a free O−H band in the IRPD

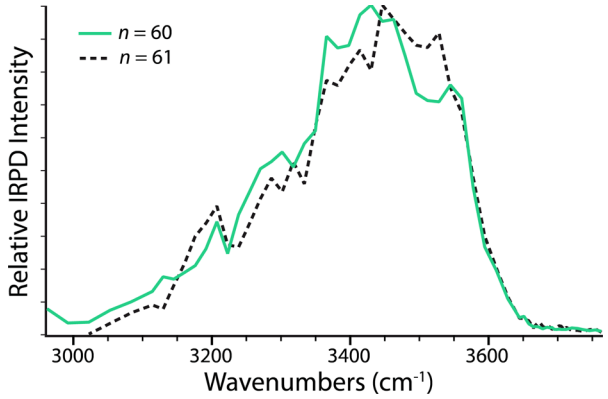

Figure 5. IRPD spectra of $Fe(CN)_6^{3-}(H_2O)_n$ n = 60 (solid green) and 61 (dotted black).

spectra of either cluster indicating that the hydrogen atoms in essentially all of the water molecules participate in hydrogen bonding for these two clusters.

Patterning of Water Molecules at Long Distances. A free O−H band is commonly observed in the spectra of hydrated ions. For cations, a free O−H band is observed from the onset of hydration, whereas for anions, this band is often only seen in the spectra of larger clusters as a result of the orientation of water molecules that interact directly with the anion. To investigate the extent to which the ferricyanide trianion affects the hydrogen-bonding network of water molecules at larger cluster size, IRPD spectra of $Fe(CN)_6^{3-}(H_2O)_n$ with n between 20 and 120 water molecules were measured at select cluster sizes (Figure 6). There is a broad band in the spectra between ~3200 and 3600 cm^{-1}, with a maximum that blue-shifts from 3521 cm^{-1} for n = 20 to 3422 cm^{-1} for n = 120. The absorption band of liquid water is centered at ~3400 cm^{-1}.[61] This suggests that the fully

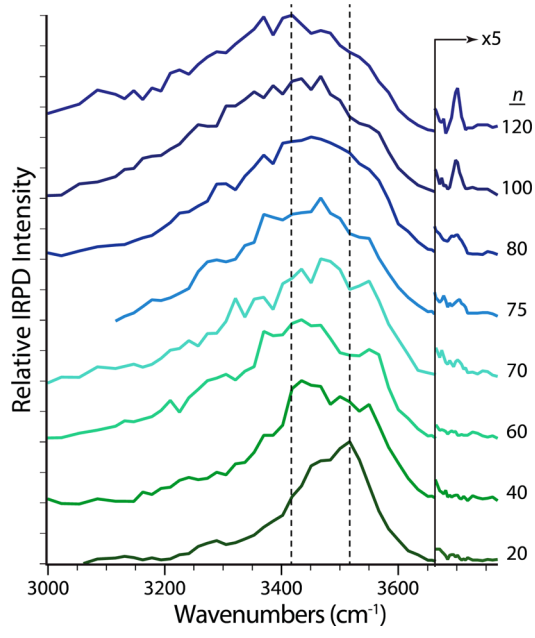

Figure 6. IRPD spectra of $Fe(CN)_6^{3-}(H_2O)_n$ with n between 20 and 120. The free O−H region has been expanded by 5× to more clearly show the band at 3700 cm^{-1} corresponding to acceptor−acceptor−donor water molecules at the surface of these clusters.

DOI: 10.1021/ja5119545
J. Am. Chem. Soc. 2015, 137, 1650−1657

hydrogen-bonded water molecules in the larger ferricyanide trianion-containing clusters are in an environment similar to that in liquid water or amorphous ice.

There is no band in the free O−H region in the smaller clusters of $Fe(CN)_6^{3-}(H_2O)_n$, indicating that all of the hydrogen atoms of water are involved in hydrogen bonds. At $n = 70$, a feature at 3707 cm^{-1} emerges, indicating the presence of water molecules with a free O−H. The intensity of this band increases with cluster size, indicating the presence of additional water molecules that have a free O−H. The frequency of this band corresponds to water molecules that are at the surface of the cluster and accept two hydrogen bonds and donate a single hydrogen bond (acceptor−acceptor−donor, or AAD, water molecules).[57−60,62−64] This frequency depends on the charge state of the ion, the cluster size, and, to a lesser extent, the size of the ion in the cluster. Results for 1− to 3+ charge state ions at $n \approx 36$, and for 2− to 3+ ions at $n \approx 250$, indicate that the frequency of this stretch is affected by the electric field at the nanodrop surface, i.e., a Stark shift, that is induced both by the charge of the ion in the cluster and by the surface potential that is caused by the net orientation of water molecules at the surface of the cluster.[65,66] This frequency also depends on the orientation of the free O−H of the water molecules at the surface.

There is a free O−H stretch for $I^-(H_2O)_n$ clusters that persists for $n > 5$.[67] In contrast, a free O−H band does not appear in the spectrum of $(H_2O)^-_n$ until $n \geq 15$[68] and until $n > 43$ for $SO_4^{2-}(H_2O)_n$.[69] The appearance of the free O−H stretch at much larger cluster sizes for SO_4^{2-} is consistent with a stronger orientation of water molecules induced by these ions as a result of the higher charge state and the formation of hydrogen bonds directly to the ion or to both the ion and to other water molecules.[70] The absence of a free O−H stretch until $n > 43$ indicates that the ion-induced effect on water orientation in the first solvation shell propagates outward into the second and even third solvation shells. This is consistent with IRPD spectroscopy of even larger SO_4^{2-} clusters that show differences in hydrogen bonding of fully hydrogen bonded water molecules even for clusters with $n \approx 250$.[66] For $Fe(CN)_6^{3-}$, the absence of the free O−H stretch for clusters with $n < 70$ shows that this ion can orient water molecules even more strongly than SO_4^{2-} and can affect the hydrogen-bonding network of water molecules as far as the fourth solvation shell.

CONCLUSIONS

Formation of small hydrated trianions, $Fe(CN)_6^{3-}(H_2O)_n$, with $n \geq 8$, directly by nESI is demonstrated. $Fe(CN)_6^{3-}$ is the smallest, highest charge density trianion that has been observed in the gas phase, and information about the structures and reactivities of these ions provides new insights into the role of water in stabilizing small multivalent anions. $Fe(CN)_6^{3-}(H_2O)_8$ dissociates by loss of an electron with BIRD. No $Fe(CN)_6^{3-}(H_2O)_7$ is observed, consistent with the absence of this and smaller hydrated trianions in the nESI mass spectra. In contrast, $Fe(CN)_6^{3-}(H_2O)_7$ is formed under the higher-energy activation conditions of IRPD, and this ion dissociates by two pathways corresponding to either loss of a water molecule or loss of an electron. The IRPD spectrum of $Fe(CN)_6^{3-}(H_2O)_8$ is consistent with computed structures in which pairs of water molecules form two hydrogen bonds directly to the ion or form one hydrogen bond to the ion and one to the other water molecule.

There are magic number clusters at $n = 58−60$, and the IRPD spectrum of the $n = 60$ cluster shows that the hydrogen atoms of all the water molecules are involved in hydrogen bonds and that these hydrogen bonds are, on average, stronger than those in the $n = 61$ cluster, which is significantly less stable. Remarkably, the IRPD spectra of these ions do not have a feature corresponding to a free O−H stretch indicating that the hydrogen atoms of all the water molecules, even those at the surface of the cluster, are involved in hydrogen bonds. IRPD spectra measured for clusters with up to 120 water molecules indicate the onset of a free O−H stretch of an acceptor-acceptor donor water molecule at the surface of the cluster occurs at $n \approx 70$, which corresponds to a droplet radius of ∼0.8 nm. These results provide compelling evidence that this trivalent ion orients water and patterns the hydrogen-bonding network of the water molecules all the way to the surface of the clusters, even for water molecules that are surrounded by other water molecules and that are not on the surface nor directly interact with the ion. These clusters are cold (133 K), and the thermal motion of water molecules is much lower than that at room temperature. Consequently, the water orientation effects of the ion will be less in liquid water. However, the forces that cause the patterning of water at low temperature still exist at higher temperature and must influence the hydrogen-bonding network of liquid water to some extent. These forces extend well past the first solvation shell and may play a role in Hofmeister and other ion-related phenomena.

Charge separation by loss of an electron from these trianions may also provide insight into why charging of many proteins and other macromolecules is less for anions than it is for cations in electrospray ionization. Loss of electrons may also occur for much larger charged droplets as solvent evaporation causes the droplets to approach the Rayleigh limit. Ejection of cationic species through an ion evaporation mechanism can occur from positively charged droplets as can loss of anionic species from anionic droplets, and these ion evaporation processes may affect charging of macromolecules.[71] Although many factors contribute to charging of macromolecules in electrospray ionization, electron loss, which would only occur significantly for anionic droplets, could result in a slightly lower charge density at the surface of anionic drops than cationic drops, and may contribute to the lower charging of many macromolecules formed as anions in ESI.

ASSOCIATED CONTENT

Supporting Information

Complete ref 48, nESI spectra from 5 mM solutions of $Na_3P_3O_9$ and $Na_3Co(NO_2)_6$, IRPD dissociation spectrum of $P_3O_9^{3-}(H_2O)_9$, structure and spectrum for **4h**, and atomic coordinates for calculated $Fe(CN)_6^{3-}(H_2O)_8$ isomers. This material is available free of charge via the Internet at http://pubs.acs.org.

AUTHOR INFORMATION

Corresponding Author

*erw@berkeley.edu

Present Address

[§]S.H.: Institute of Inorganic and Analytical Chemistry, Justus-Liebig-University Giessen, 35392 Giessen, Germany

Notes

The authors declare no competing financial interest.

DOI: 10.1021/ja5119545
J. Am. Chem. Soc. 2015, 137, 1650−1657

■ ACKNOWLEDGMENTS

The authors thank the National Science Foundation (grant CHE-1306720) for generous financial support of this research and are grateful to the German National Academy of Sciences Leopoldina (LPDS 2012−15) for a postdoctoral scholarship and financial support (S.H.).

■ REFERENCES

(1) Boldyrev, A. I.; Gutowski, M.; Simons, J. *Acc. Chem. Res.* **1996**, *29*, 497−502.
(2) Hampe, O.; Neumaier, M.; Blom, M. N.; Kappes, M. M. *Chem. Phys. Lett.* **2002**, *354*, 303−309.
(3) Petrie, S.; Wang, J.; Böhme, D. K. *Chem. Phys. Lett.* **1993**, *204*, 473−480.
(4) Williams, E. R. *J. Mass Spectrom.* **1996**, *31*, 831−842.
(5) Yoo, H. J.; Wang, N.; Zhuang, S.; Song, H.; Håkansson, K. *J. Am. Chem. Soc.* **2011**, *133*, 16790−16793.
(6) Wang, X. B.; Wang, L. S. *Annu. Rev. Phys. Chem.* **2009**, *60*, 105−126.
(7) Schröder, D.; Schwarz, H. *J. Phys. Chem. A* **1999**, *103*, 7358−7394.
(8) Boxford, W. E.; Dessent, C. E. H. *Phys. Chem. Chem. Phys.* **2006**, *8*, 5151−5165.
(9) Danell, A. S.; Parks, J. H. *J. Am. Soc. Mass Spectrom.* **2003**, *14*, 1330−1339.
(10) Wang, X. B.; Sergeeva, A. P.; Xing, X. P.; Massaouti, M.; Karpuschkin, T.; Hampe, O.; Boldyrev, A. I.; Kappes, M. M.; Wang, L. S. *J. Am. Chem. Soc.* **2009**, *131*, 9836−9842.
(11) Arnold, K.; Balaban, T. S.; Blom, M. N.; Ehrler, O. T.; Gilb, S.; Hampe, O.; Lier, J. E.; Weber, J. M.; Kappes, M. M. *J. Phys. Chem. A* **2003**, *107*, 794−803.
(12) Wong, R. L.; Williams, E. R. *J. Phys. Chem. A* **2003**, *107*, 10976−10983.
(13) Blades, A. T.; Kebarle, P. *J. Am. Chem. Soc.* **1994**, *116*, 10761−10766.
(14) Gao, B.; Liu, Z. *J. Chem. Phys.* **2005**, *123*, No. 224302.
(15) Wang, X. B.; Nicholas, J. B.; Wang, L. S. *J. Chem. Phys.* **2000**, *113*, 10837−10840.
(16) Schauer, S. N.; Williams, P.; Compton, R. N. *Phys. Rev. Lett.* **1990**, *65*, 625−628.
(17) Puškar, L.; Tomlins, K.; Duncombe, B.; Cox, H.; Stace, A. J. *J. Am. Chem. Soc.* **2005**, *127*, 7559−7569.
(18) Blades, A. T.; Jayaweera, P.; Ikonomou, M. G.; Kebarle, P. *Int. J. Mass Spectrom. Ion Processes* **1990**, *102*, 251−267.
(19) Shvartsburg, A. A.; Siu, K. W. M. *J. Am. Chem. Soc.* **2001**, *123*, 10071−10075.
(20) Cooper, T. E.; Armentrout, P. B. *J. Phys. Chem. A* **2009**, *113*, 13742−13751.
(21) Bush, M. F.; Saykally, R. J.; Williams, E. R. *Int. J. Mass Spectrom.* **2006**, *253*, 256−262.
(22) McQuinn, K.; Hof, F.; McIndoe, J. S. *Chem. Commun.* **2007**, *40*, 4099−4101.
(23) Gross, D. S.; Rodriguez-Cruz, S. E.; Bock, S.; Williams, E. R. *J. Phys. Chem.* **1995**, *99*, 4034−4038.
(24) Feil, S.; Koyanagi, G. K.; Böhme, D. K. *Int. J. Mass Spectrom.* **2009**, *280*, 38−41.
(25) Spears, K. G.; Fehsenfeld, F. C. *J. Chem. Phys.* **1972**, *56*, 5698−5705.
(26) Spears, K. G.; Fehsenfeld, G. C.; McFarland, M.; Ferguson, E. E. *J. Chem. Phys.* **1972**, *56*, 2562−2566.
(27) Beyer, M.; Williams, E. R.; Bondybey, V. E. *J. Am. Chem. Soc.* **1999**, *121*, 1565−1573.
(28) Stace, A. J. *J. Phys. Chem. A* **2002**, *106*, 7993−8005.
(29) Wang, L. S.; Ding, C. F.; Wang, X. B.; Nicholas, J. B. *Phys. Rev. Lett.* **1998**, *81*, 2667−2670.
(30) Roithová, J.; Schwarz, H.; Schröder, D. *Chem.—Eur. J.* **2009**, *15*, 9995−9999.
(31) Blom, M. N.; Hampe, O.; Gilb, S.; Weis, P.; Kappes, M. M. *J. Chem. Phys.* **2001**, *115*, 3690−3697.
(32) Cox, H.; Akibo-Betts, G.; Wright, R.; Walker, N.; Curtis, S.; Duncombe, B.; Stace, A. J. *J. Am. Chem. Soc.* **2003**, *125*, 233−242.
(33) Wright, R.; Walker, N.; Firth, S.; Stace, A. J. *J. Phys. Chem. A* **2001**, *105*, 54−64.
(34) Whitehead, A.; Barrios, R.; Simons, J. *J. Chem. Phys.* **2002**, *116*, 2848−2851.
(35) Schröder, D.; Schwarz, H.; Wu, J.; Wesdemiotis, C. *Chem. Phys. Lett.* **2001**, *343*, 258−264.
(36) Böhme, D. K. *Phys. Chem. Chem. Phys.* **2011**, *13*, 18253−18263.
(37) Kordel, M.; Schooss, D.; Gilb, S.; Blom, M. N.; Hampe, O.; Kappes, M. M. *J. Phys. Chem. A* **2004**, *108*, 4830−4837.
(38) Dau, P. D.; Liu, H. T.; Yang, J. P.; Winghart, M. O.; Wolf, T. J. A.; Unterreiner, A. N.; Weis, P.; Miao, Y. R.; Ning, C. G.; Kappes, M. M.; Wang, L. S. *Phys. Rev. A* **2012**, *85*, 064503.
(39) Wang, X. B.; Yang, X.; Nicholas, J. B.; Wang, L. S. *Science* **2001**, *294*, 1322−1325.
(40) Xin, Y.; Wang, X. B.; Wang, L. S. *J. Phys. Chem. A* **2002**, *106*, 7607−7616.
(41) Žabka, J.; Ricketts, C. L.; Schröder, D.; Roithová, J.; Schwarz, H.; Thissen, R.; Dutuit, O.; Price, S. D.; Herman, Z. *J. Phys. Chem. A* **2010**, *114*, 6463−6471.
(42) Lee, S.-W.; Freivogel, P.; Schindler, T.; Beauchamp, J. L. *J. Am. Chem. Soc.* **1998**, *120*, 11758−11765.
(43) Rodrigez-Cruz, S. E.; Klassen, J. S.; Williams, E. R. *J. Am. Soc. Mass Spectrom.* **1999**, *10*, 958−968.
(44) Zhang, X.; Wanigasekara, E.; Breitbach, Z. S.; Dodbiba, E.; Armstrong, D. W. *Rapid Commun. Mass Spectrom.* **2010**, *24*, 1113−1123.
(45) Bush, M. F.; O'Brien, J. T.; Prell, J. S.; Saykally, R. J.; Williams, E. R. *J. Am. Chem. Soc.* **2007**, *129*, 1612−1622.
(46) Wong, R. L.; Paech, K.; Williams, E. R. *Int. J. Mass Spectrom.* **2004**, *232*, 59−66.
(47) Prell, J. S.; O'Brien, J. T.; Williams, E. R. *J. Am. Soc. Mass Spectrom.* **2010**, *21*, 800−809.
(48) Shao, Y.; et al. *Phys. Chem. Chem. Phys.* **2006**, *8*, 3172−3191.
(49) Chang, T. M.; Prell, J. S.; Warrick, E. R.; Williams, E. R. *J. Am. Chem. Soc.* **2012**, *134*, 15805−15813.
(50) Davis, D. D.; Okabe, H. *J. Chem. Phys.* **1968**, *49*, 5526−5531.
(51) Bradforth, S. E.; Kim, E. H.; Arnold, D. W.; Neumark, D. M. *J. Chem. Phys.* **1993**, *98*, 800−810.
(52) Ma, L.; Majer, K.; Chirot, F.; Issendorff, B. *J. Chem. Phys.* **2009**, *131*, No. 144303.
(53) Knapp, M.; Echt, O.; Kreisle, D.; Recknagel, E. *J. Phys. Chem.* **1987**, *91*, 2601−2607.
(54) Kondow, T.; Nagata, T.; Kuchitsu, K. *Z. Phys. D: At., Mol. Clusters* **1989**, *12*, 291−292.
(55) Gruenloh, C. J.; Carney, J. R.; Arrington, C. A.; Zwier, T. S.; Fredericks, S. Y.; Jordan, K. D. *Science* **1997**, *276*, 1678−1681.
(56) Miyazaki, M.; Fujii, A.; Ebata, T.; Mikami, N. *Science* **2004**, *304*, 1134−1137.
(57) Shin, J. W.; Hammer, N. I.; Diken, E. G.; Johnson, M. A.; Walters, R. S.; Jaeger, T. D.; Duncan, M. A.; Christie, R. A.; Jordan, K. D. *Science* **2004**, *304*, 1137−1140.
(58) Cooper, R. J.; Chang, T. M.; Williams, E. R. *J. Phys. Chem. A* **2013**, *117*, 6571−6579.
(59) Fournier, J. A.; Johnson, C. J.; Wolke, C. T.; Weddle, G. H.; Wolk, A. B.; Johnson, M. A. *Science* **2014**, *344*, 1009−1012.
(60) Fournier, J. A.; Wolke, C. T.; Johnson, C. J.; Johnson, M. A.; Heine, N.; Gewinner, S.; Schöllkopf, W.; Esser, T. K.; Fagiani, M. R.; Knorke, H.; Asmis, K. R. *Proc. Natl. Acad. Sci. U.S.A.* **2014**, *111*, 18132−18137.
(61) Freda, M.; Piluso, A.; Santucci, A.; Sassi, P. *Appl. Spectrosc.* **2005**, *59*, 1155−1159.
(62) Headrick, J. M.; Diken, E. G.; Walters, R. S.; Hammer, N. I.; Christie, R. A.; Cui, J.; Myshakin, E. M.; Duncan, M. A.; Johnson, M. A.; Jordan, K. D. *Science* **2005**, *308*, 1765−1769.

DOI: 10.1021/ja5119545
J. Am. Chem. Soc. 2015, 137, 1650−1657

(63) Diken, E. G.; Hammer, N. I.; Johnson, M. A.; Christie, R. A.; Jordan, K. D. *J. Chem. Phys.* **2005**, *123*, No. 164309.
(64) Walters, R. S.; Pillai, E. D.; Duncan, M. A. *J. Am. Chem. Soc.* **2005**, *127*, 16599−16610.
(65) Prell, J. S.; O'Brien, J. T.; Williams, E. R. *J. Am. Chem. Soc.* **2011**, *133*, 4810−4818.
(66) O'Brien, J. T.; Williams, E. R. *J. Am. Chem. Soc.* **2012**, *134*, 10228−10236.
(67) Ayotte, P.; Bailey, C. G.; Weddle, G. H.; Johnson, M. A. *J. Phys. Chem. A* **1998**, *102*, 2067−3071.
(68) Hammer, N. I.; Roscioli, J. R.; Bopp, J. C.; Headrick, J. M.; Johnson, M. A. *J. Chem. Phys.* **2005**, *123*, No. 244311.
(69) O'Brien, J. T.; Prell, J. S.; Bush, M. F.; Williams, E. R. *J. Am. Chem. Soc.* **2010**, *132*, 8248−8249.
(70) Bush, M. F.; Saykally, R. J.; Williams, E. R. *J. Am. Chem. Soc.* **2007**, *129*, 2220−2221.
(71) Hogan, C. J.; Carroll, J. A.; Rohrs, H. W.; Biswas, P.; Gross, M. L. *Anal. Chem.* **2009**, *81*, 369−377.

DOI: 10.1021/ja5119545
J. Am. Chem. Soc. 2015, 137, 1650−1657